Chapter II

Diferric oxo-bridged Complexes with Polydentate Aminopyridyl Ligand bpmen: Synthesis, Structure and Catalytic Reactivity*

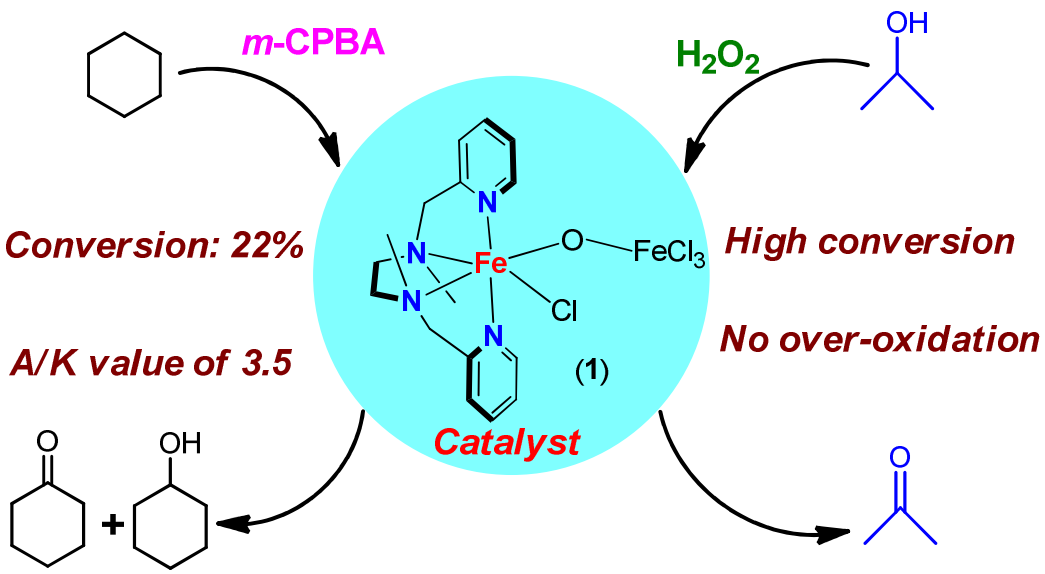

*Published in *Transition Metal Chemistry*, 39: 909-915 (**2014**).

Chapter II

Abstract

The catalytic reactivity of a group of diferric oxo-bridged complexes (**1**-**3**) of tetradentate bpmen ligand (bpmen= N,N'-dimethyl-N,N'-bis(2-pyridylmethyl)-ethane-1,2-diamine) towards alkane hydroxylation has been evaluated. Among the three complexes, the μ-oxo diiron(III) complex [Fe(bpmen)(μ-O)$FeCl_3$] (**1**) has been synthesized for the very first time. The complex **1** has been characterized by spectroscopic analysis and X-ray crystallography. At room temperature the μ-oxo diiron(III) complexes [**1**-**3**] have been found to be useful catalysts in hydroxylation of alkanes with *m*-chloroperbenzoic acid as oxidant. [Fe(bpmen)(μ-O)$FeCl_3$] (**1**) has been found to be the most active catalyst. Moreover, the catalytic ability of the complexes in the oxidation of alcohols to ketones with mild hydrogen peroxide at room temperature has also been investigated.

II.1. Introduction

Non-heme diiron centers bridged by oxo (or hydroxo) and carboxylato groups have attracted a great deal of interest among bioinorganic chemists over the past two decades [1-3]. Given the higher stability of the μ-oxo diiron(III) motif, it is not surprising that nature has chosen this motif as the active sites of several proteins [4-9]. The μ-oxo diiron(III) unit has been found in several non-heme enzymes which include methane monooxygenase (MMO) [5,6], ribonucleotide reductase (RNR) [7,8] and fatty acid desaturases [9]. These enzymes carry out diverse biological reactions such as hydroxylation of methane (MMO), toluene (toluene-4-monooxygenase), generation of tyrosine radical (RNR), desaturation of saturated fatty acids. These fascinating pattern of reactivity shown by of the μ-oxo diiron(III) motif present in the enzymes has stimulated efforts to develop analogues in model systems to provide a chemical basis for understanding the reactivity of the metalloenzymes. Over the last two decades, several complexes with μ-oxo diiron(III) unit have been synthesized and characterized [1, 10-15]. Depending upon the bite angle of the nitrogen rich ligands employed, μ-oxo diferric complexes with Fe-O-Fe angles ranging from 180° to 114° have been obtained [10]. In this regard, tetradentate tripodal ligands such as TPA (TPA= tris-(2-pyridylmethyl)amine) and linear tetradentate ligands such as bpmen (bpmen = N,N'-dimethyl-N,N'-bis(2-pyridylmethyl)-ethane-1,2-diamine) have been explored in designing a variety of dinuclear metal complexes [1, 11, 15]. In particular doubly bridged oxo/hydroxo diferric complexes based on TPA have emerged as excellent structural models for compound Q of sMMO [14]. On the other hand, μ-oxo diferric complexes based on bpmen ligand [11,15] have received much less attention in this regard/area, although few well characterized complexes were reported but the investigation on their catalytic ability is only limited to the epoxidation of alkenes [15f]. So far, no report on the catalytic behavior of μ-oxo diferric complexes of bpmen ligand towards hydroxylation of alkanes is available in the literature. This prompted us to undertake a detailed study on the catalytic behavior of μ-oxo diferric complexes of bpmen ligand towards room temperature hydroxylation of alkanes. A group of μ-oxo (**1**), (μ-oxo)(μ-hydroxo) (**2**) [15] and (μ-oxo)(μ-acetato) (**3**) [11] bridged diiron(III)

complexes based on bpmen ligand has been chosen to examine their catalytic ability towards room temperature alkane hydroxylation with *m*-chloroperbenzoic acid. The μ-oxo diiron(III) complexes (**1**-**3**) differ in their coordination environment around iron(III) centres as well as the Fe-O-Fe angles (Scheme II.1). The complex [Fe(bpmen)(μ-O)$FeCl_3$] (**1**) containing a linear Fe-O-Fe unit has been synthesized for the first time and structurally characterized. Moreover, the catalytic efficacy of the above complexes has been further compared in oxidation of benzyl alcohols at room temperature with mild hydrogen peroxide.

II.2. Result and discussion

II.2.1. Synthesis

The ligand bpmen (bpmen = N,N'-dimethyl-N,N'-bis(2-pyridylmethyl)-ethane-1,2-diamine) was synthesized according to the reported [15a] procedure. The neutralization of 2-chloromethyl pyridine chloride hydrochloride with aqueous potassium carbonate followed by the reaction with N,N'-dimethyl ethylene diamine in presence of sodium hydroxide after 48 hours stirring afford the compound as orange oil. The synthesized ligand has been characterized by ^{1}H NMR and ESI-MS techniques. The synthetic procedures for the μ-oxo diiron(III) complexes (**1**-**3**) has been outlined in Scheme II.1.

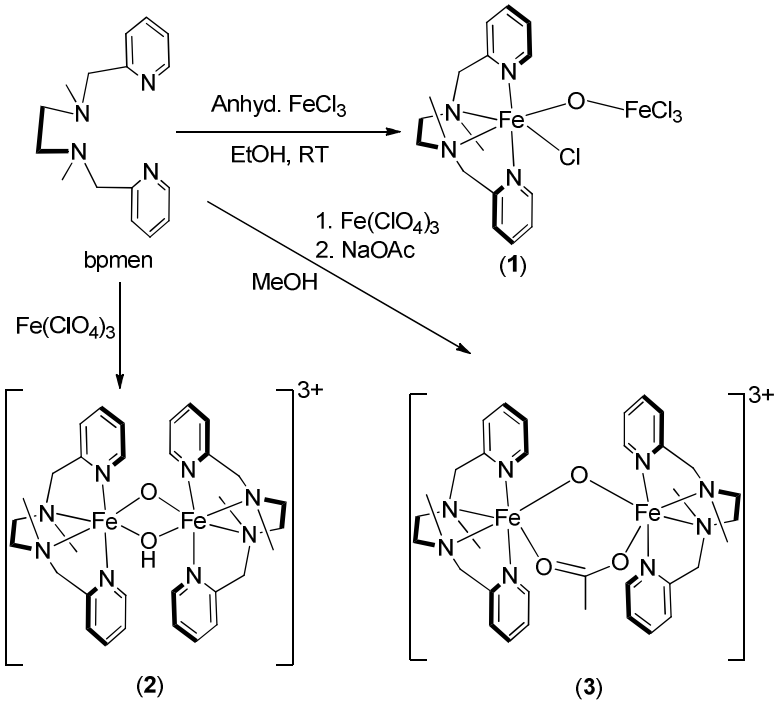

Scheme II.1 Synthetic routes to complexes **1**-**3**.

Reaction of equimolar amounts of bpmen and anhydrous $FeCl_3$ in ethanol under aerobic condition afforded the μ-oxo diiron(III) complex **1**. The other two complexes (**2** and **3**) have been synthesized by following the procedure already reported in the literature [15b, 11]. The complex **2** was synthesized by mixing ferric perchlorate solution in ethanol to an ethanolic solution of ligand and sodium hydroxide in ethanol. The deep brown solution was kept in refrigerator for overnight. A deep maroon precipitate was obtained which was filtered, washed thoroughly with ether and air dried. Complex **3** was synthesized by mixing ferric chlorate dissolved in methanol to a solution of bpmen ligand and sodium acetate dissolved in methanol and water. The product was precipitated as brown powder. It was filtered, washed thoroughly with cold methanol and air dried.

II.2.2. Characterisation

II.2.2.1. ^{1}H NMR spectra

The synthesized ligand has been characterized by ^{1}H NMR technique. The spectral data of the ligand is given in the experimental section and it is fully matched with the literature value [15a]. The NMR spectrum of the ligand is shown in the Figure II.1.

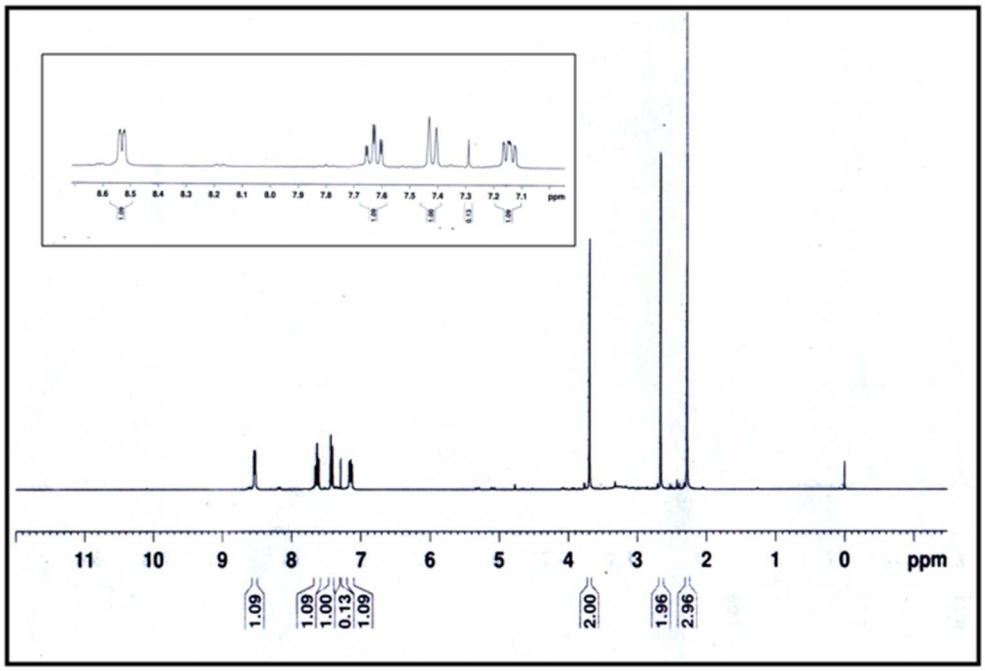

Fig II.1 ^{1}H NMR spectra of the ligand bpmen; Inset: Expanded aromatic region.

II.2.2.2. Electronic spectra

Electronic spectra of the complex **1** and **2** together with the corresponding (μ-oxo)(μ-acetato)diiron(III)complex (**3**) recorded in acetonitrile at room temperature are shown in Fig II.2. UV-Vis absorption properties of μ-oxo diiron(III) complexes have been shown to be dependent on their Fe-O-Fe angles. Complexes containing linear Fe-O-Fe unit normally show bands in the 600-700 nm region and are assignable to oxo-to-iron(III) charge transfer transitions. As the Fe-O-Fe angles decrease such bands shift towards lower wavelengths [15e]. Moreover, the intensities of bands in the 400-550 nm regions increase when the Fe-O-Fe angles become more and more acute. This trend is well maintained in the symmetrical diiron(III) complexes **2** and **3**. However, no absorption corresponding to oxo-to-iron(III) charge transfer is obtained in case of complex **1**, which can be attributed to the asymmetric coordination environment around the two iron(III) centres.

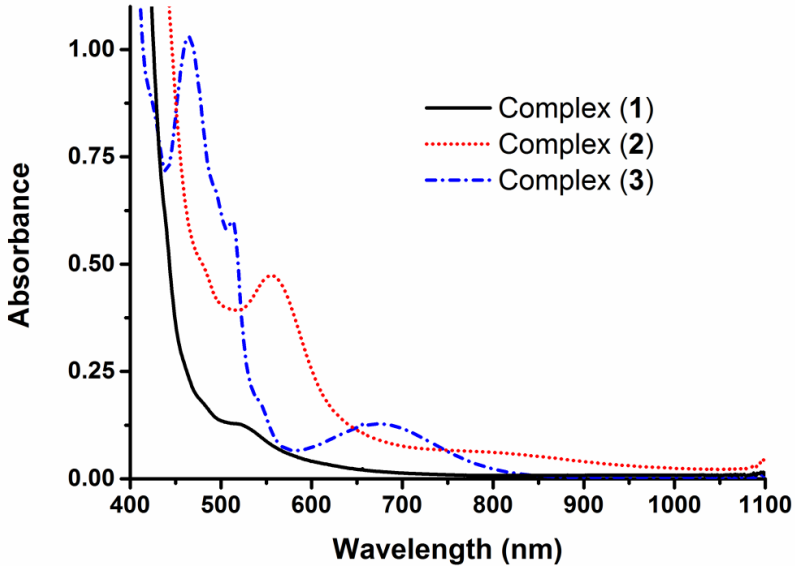

Fig II.2 UV-Vis spectra of the complexes (**1**-**3**) in acetonitrile at room temperature (concentration of the complexes = 1.0 mM).

The UV-Vis spectra of complex **1** exhibits an intense feature at 250 nm which is associated to a pyridyl π- π* transition and the second feature around 300-400 nm is assignable to the transitions arise from ligand to metal charge transfer transition i.e. LMCT which is independent of Fe-O-Fe angle. Therefore the transitions at 339 and 400 nm are due to ligand-to-metal charge transfer transitions [16]. The less intense band at 400 nm is assigned to the $^6A_1 \rightarrow$ ($^4A_1$, ^4E) transition and is the signature of

the Fe-(μ-O)-Fe motif, suggesting that the dinuclear structure is maintained in solution of acetonitrile (Fig II.3) [11].

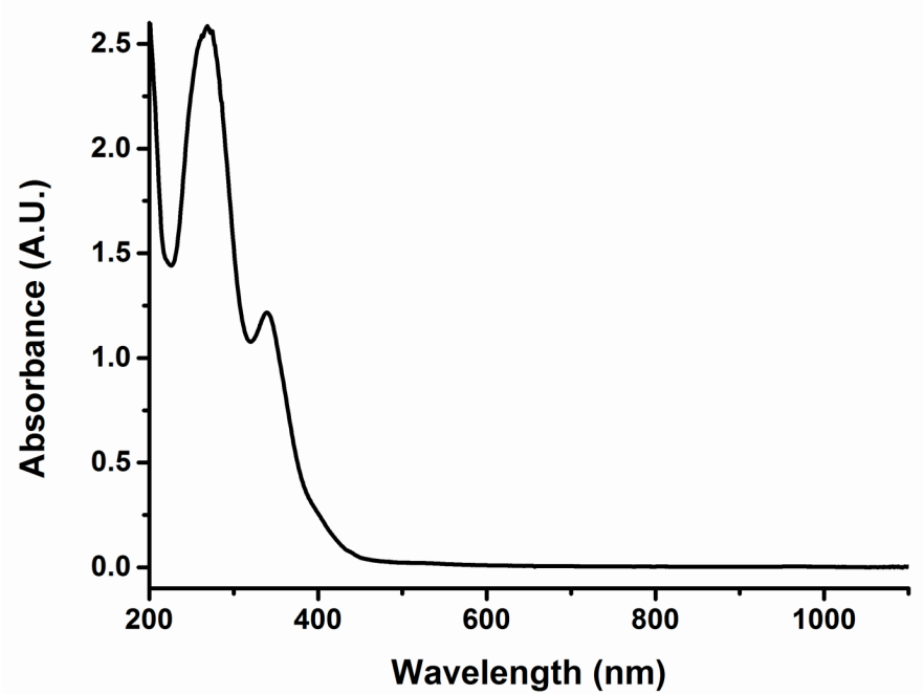

Fig II.3 UV-Vis spectra of the complex **1** in acetonitrile at room temperature (concentration of the complex = 1.0 mM).

II.2.2.3. ESI-MS spectra

The complex **2** and **3** have been characterised by ESI-MS and elemental analysis. Detailed experimental procedures and characterisation are compiled in the experimental section. Representative ESI-MS spectrums of the complexes **2** & **3** are given in the Figure II.4 and Figure II.5 respectively. The complex **2** has a prominent peak at m/z 392, which corresponds to $[Fe(bpmen)(\mu\text{-}O)(\mu\text{-}OH)Fe(bpmen)]^{+3}$. The corresponding ESI-MS spectra of complex **2** is given in Fig II.4. On the other hand the complex **3** has a major peak at m/z 413 which is attributed for the species $[Fe(bpmen)(\mu\text{-}O)(\mu\text{-}OAc)Fe(bpmen)](ClO_4)]^{+2}$. The ESI-MS spectrum of the complex **3** is shown in the Fig II.5

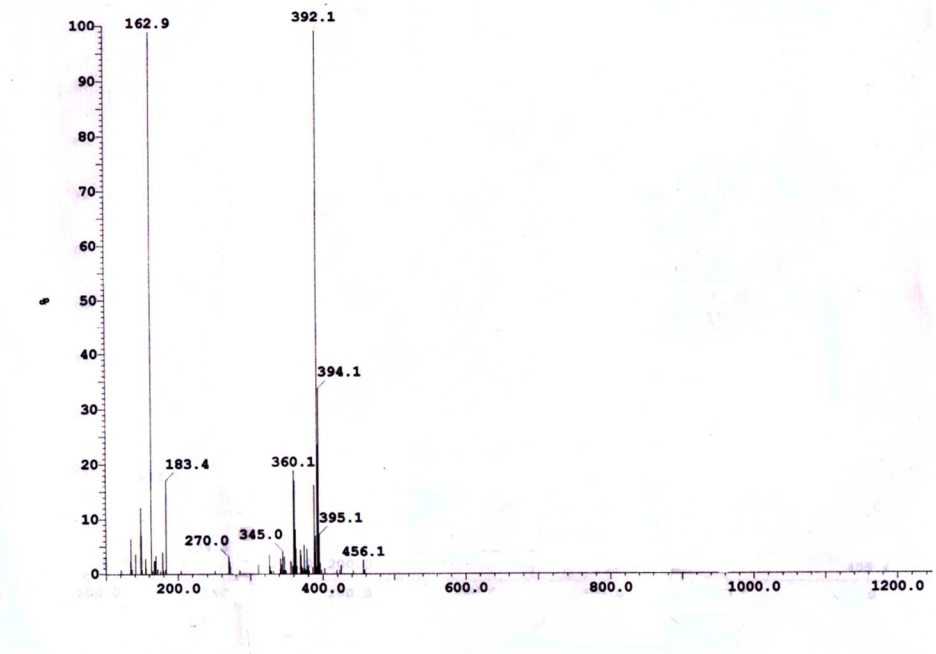

Fig II.4 ESI-MS spectra of the complex [Fe(bpmen)(µ-O)(µ-OH)Fe(bpmen)]$(ClO_4)_3$ **(2)**.

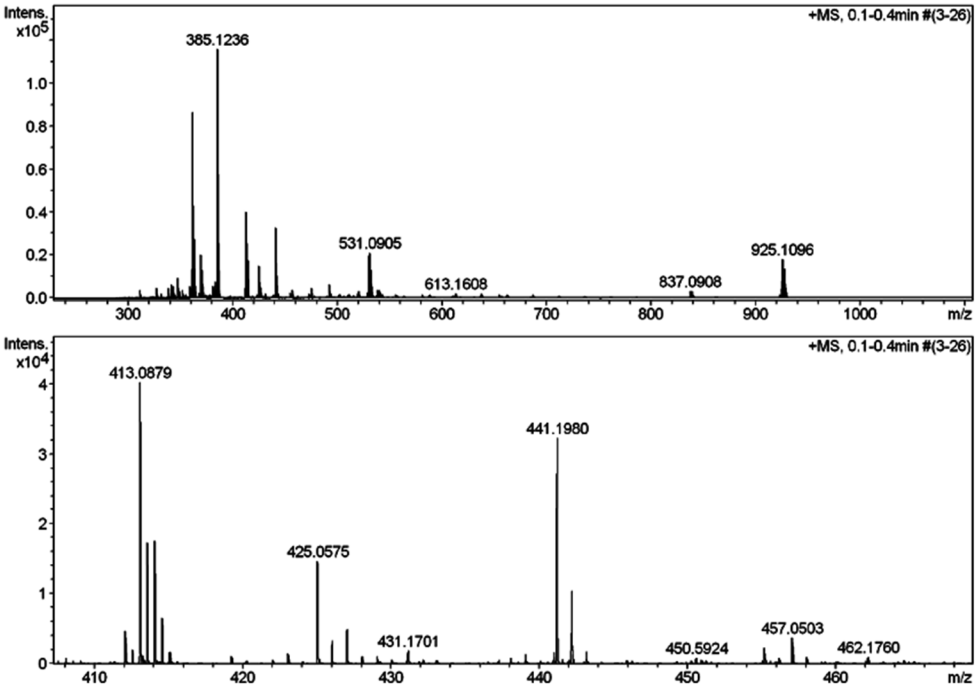

Fig II.5 ESI-MS spectra of the complex [Fe(bpmen)(µ-O)(µ-CH_3COO)Fe(bpmen)]$(ClO_4)_3$**(3)**.

II.2.2.4. X-ray Crystallography

All the complexes have been characterized by elemental analysis and ESI-MS studies. Moreover, the solid state structure of complex **1** has been confirmed by single crystal X-ray diffraction. The molecular structure of the complex **1** is shown in Fig II.6. Selected bond parameters and crystal information data are collected in Table II.1 and Table II.2 respectively.

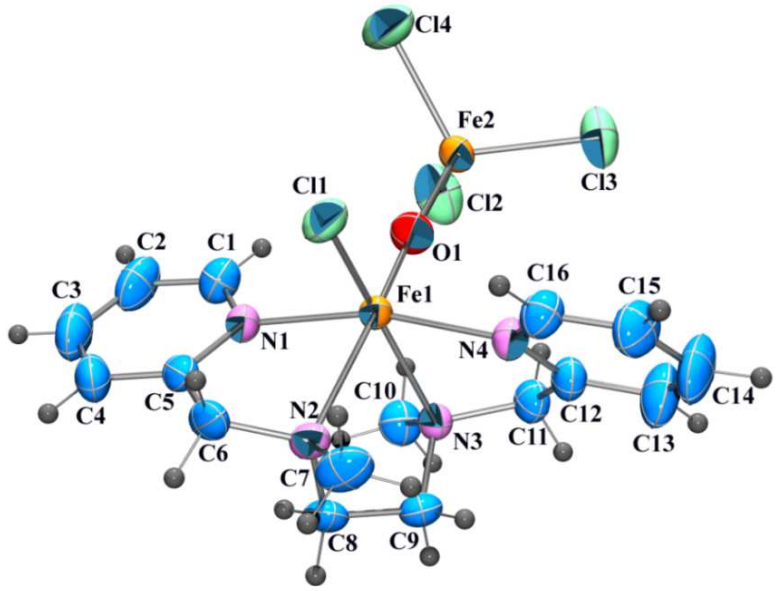

Fig II.6 Ortep plot of the complex **1** [Fe(bpmen)(μ-O)$FeCl_3$] showing 50% probability ellipsoids.

Table II.1 Selected bond lengths (Å) and bond angles (°) for the complex **1**.

Bond lengths(Å)		Bond angles (°)	
Fe(1)-μ-O(1)	1.788(2)	Fe1-(μ-O1)-Fe2	171.99(15)
Fe(2)-μ-O(1)	1.752(2)	O(1)-Fe(1)-N(4)	97.42(10)
Fe(1)-N(1)	2.172(2)	O(1)-Fe(1)-N(1)	93.24(10)
Fe(1)-N(4)	2.165(2)	N(4)-Fe(1)-N(1)	165.53(10)
Fe(1)-N(2)	2.279(3)	O(1)-Fe(1)-N(3)	75.07(9)
Fe(1)-N(3)	2.239(3)	N(1)-Fe(1)-N(3)	95.27(10)
Fe(2)-Cl(2)	2.2252(12)	O(1)-Fe(1)-Cl(1)	103.56(9)
Fe(2)-Cl(3)	2.2099(10)	O(1)-Fe(2)-Cl(3)	111.24(8)
Fe(2)-Cl(4)	2.2180(12)	O(1)-Fe(2)-Cl(4)	109.35(8)
		Cl(3)-Fe(2)-Cl(4)	110.12(5)
		O(1)-Fe(2)-Cl(2)	110.48(9)
		Cl(3)-Fe(2)-Cl(2)	107.24(4)
		Cl(4)-Fe(2)-Cl(2)	108.35(5)

Table II.2 Crystallographic data and processing parameters for complex **1**.

Identification code	Complex (**1**)
Chemical formula	$C_{16}H_{22}Cl_4Fe_2N_4O$
Formula weight	539.88
Temperature	293(2) K
Wavelength	0.71073 Å
Crystal System, space group	Monoclinic, P(2)1/c
Unit cell dimensions	a = 31.551(6) Å
	b = 10.670(2) Å
	c = 14.130(3) Å
	α = 90°
	β = 102.226(3)°
	γ = 90°
Volume	4648.8(16) $Å^3$
Z, Calculated density	8, 1.543 mg m^{-3}
Absorption coefficient	1.721 mm^{-1}
F(000)	2192
Crystal size	0.25 x 0.16 x 0.11 mm
θ range for data collection	1.98 to 25.00 deg.
Limiting indices	
Reflections collected / unique	44314 / 8190 [R(int) = 0.1837]
Completeness to theta	25.00 99.9 %
Refinement method	Full-matrix least-squares on F^2
Data / restraints / parameters	8190 / 0 / 491
Goodness-of-fit on F^2	1.012
Final R indices [I>2σ (I)][a,b]	R1 = 0.0420, wR2 = 0.1092
R indices (all data)	R1 = 0.0518, wR2 = 0.1130
Largest diff. peak and hole	

[a]$R1= (\Sigma||F_0|-|F_c||) /(\Sigma|F_0|)$. [b]$wR2= [\Sigma w(F_0^2-F_c^2)^2 / \Sigma w(F_0^2)^2]^{1/2}$

The crystal structure of **1** reveals two chemically identical complexes with almost identical geometries per asymmetric unit. The differic complex is comprised of two iron atoms with nonequivalent coordination spheres, in which Fe1 is six-coordinated in a pseudo-octahedral environment and Fe2 is tetra-coordinated. The two iron atoms are bridged by the oxo donor. Two pyridyl nitrogen atoms (N1 and N4), the two nitrogen atoms from the tertiary amines of the ligand bpmen (N2 and N3) and a chloride ligand constitute the coordination sphere of Fe1. In contrast, Fe2 is coordinated to the oxo donor and three chlorides. The presence of a linear μ-oxo diiron(III) unit in Complex **1** is reflected by the Fe–O–Fe bond angle of 171.21(15) with an Fe–Fe distance of 3.531 Å , which is considerably longer than that obtained for the (μ-oxo) (μ-hydroxo)diiron(III) complex (**2**) (Table II.2) [15b]. The Fe-μ-O

bond lengths in **1** are typical of such bonds reported in the literature (1.788(2) and 1.752(2) Å, respectively). As expected, the Fe–N_{py} bond lengths (average 2.17 Å) are shorter than the Fe–N_{amine} distances (average 2.26 Å).

The selected bond lengths and bond angles for the complexes **1, 2, 3** are compared in Table II.3.

Table II.3 Selected bond lengths (Å) and bond angles (º) for the complexes (**1–3)**:

	1[a]	**2**[b]	**3**[c]
Fe(1)…Fe(2)	3.531 (4)	2.8212 (19)	3.253 (1)
Fe(1)–μ-O(1)	1.784 (2)	1.884 (4)	1.804 (3)
Fe(2)–μ-O(1)	1.755 (2)	1.892 (4)	1.804 (3)
Fe(1)–N(1)	2.145 (2)	2.115 (5)	2.156 (6)
Fe(1)–N(4)	2.159 (2)	2.124 (5)	2.143 (6)
Fe(1)–N(2)	2.277 (3)	2.215 (5)	2.205 (6)
Fe(1)–N(3)	2.239 (3)	2.226 (5)	2.260 (6)
Bond angles (°)			
Fe1–(μ-O1)-Fe2	171.21 (15)	96.68 (19)	128.7 (4)

[a] Each asymmetric unit contains two independent molecules; [b] Ref. [15b]; [c] Ref. [15d].

II.2.3. Catalytic performance of μ-oxo diiron(III) complexes

II.2.3.1. Hydroxylation of alkanes

The catalytic efficacy of the μ-oxo diiron(III) complexes (**1**-**3**) has been evaluated towards activation of unactivated C-H bonds, such as those in cycloalkanes. Given the higher bond dissociation energies of cycloalkanes (99.3 kcal/mole in case of cyclohexane), activation of C(sp^3)-H bonds is extremely challenging [16, 17]. The performance of the complexes in alkane hydroxylation at room temperature with *m*-CPBA as the oxidant has been compiled in Table II.4. As evident from Table II.4, the unsymmetric μ-oxo diiron(III) complex **1** emerges as a modest catalyst in alkane hydroxylation at room temperature.

Table II.4 Oxidation of alkanes by *m*-CPBA catalyzed by complexes **1**-**3** at room temperature[a].

Entry	Substrate	Catalyst	Products (% yield)[b]	A/K	3°/2°
1	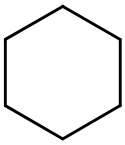	1	Cyclohexanol (17) Cyclohexanone (05)	3.4	-
2		2	Cyclohexanol (09) Cyclohexanone (03)	3.0	-
3		3	Cyclohexanol (17) Cyclohexanone (04)	4.3	-
4	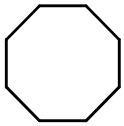	1	Cyclooctanol (25) Cyclooctanone (07)	3.5	-
5		2	Cyclooctanol (11) Cyclooctanone (04)	2.75	-
6		3	Cyclooctanol (20) Cyclooctanone (06)	3.3	-
7	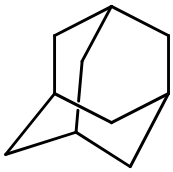	1	Adamantan-1-ol (25) Adamantan-2-ol (02) Adamantan-2-one (04)	-	12.5
8		2	Adamantan-1-ol (12) Adamantan-2-ol (02) Adamantan-2-one (01)	-	12
9		3	Adamantan-1-ol (22) Adamantan-2-ol (03) Adamantan-2-one (02)	-	13.2

[a]Reaction Condition: 0.7mM catalyst, 700mM substrate, 70 mM *m*-CPBA in acetonitrile (in case of adamantane, 2:3 acetonitrile/dichloromethane, *v/v* was used as solvent) at room temperature; [b]Yields are reported with respect to the initial concentration of the oxidant.

With a catalyst: oxidant: substrate molar ratio of 1:100:1000, the oxidation of cyclohexane has been found to be completed within an hour. Catalytic work-up and GC analysis showed the generation of cyclohexanol and cyclohexanone as the oxidation products. Conversion around 22% was observed with a higher selectivity for the alcohol product (A/K = 3.4). Under identical reaction condition, complex **3** has shown similar activity in cyclohexane oxidation affording 21% oxygenates (A/K =3.0) in 1h. In contrast, complex **2** has been found to be much less reactive in cyclohexane oxidation (Entry 2, Table II.4). Similar results are obtained in case of cyclooctane oxidation. It is interesting to note that complex (**2**) was found to be much superior catalyst to complex (**3**) in olefin epoxidation [15f]. In order to gain further insight, the reaction of complex **2** with *m*-CPBA in presence of cyclohexane

has been monitored by UV-Vis spectroscopy. Upon addition of *m*-CPBA to the reaction mixture containing complex **2** (1.0 mM) and cyclohexane in acetonitrile leads to the appearance of a band around 615 nm. Identical spectral changes have been observed in absence of substrate. The observation is indicative of the formation of the salicylate bound iron(III) complex formed *via ortho*-hydroxylation of *m*-CPBA akin to what observed in reactions of mononuclear non-heme iron(II) complexes with *m*-CPBA [18]. Indeed, after acetylation of the bluish green reaction mixture with acetic anhydride and 1-methyl imidazole [18] and GC analysis confirms the presence of 3-chlorosalicylic acid (0.4 TN) in the present case. Thus, catalytic hydroxylation and *ortho*-hydroxylation of *m*-CPBA have been found to be competitive in this case, which in turn justifies the lower catalytic efficiency of **2** in alkane hydroxylation.

The catalytic property of the complexes has also been studied in the oxidation of adamantane (Entries 7-9, Table II.4). The catalytic activity of the diiron(III) complexes towards oxidation of adamantane follows the trend **1**>**3**>**2**. In case of catalyst **1**, adamantane has been found to get oxidized to a mixture of 1-adamantanol (25%), 2-adamantanol (02%) and 2-adamantanone (04%). The normalized 3°/2° ratio in this case has been found to be 12.5. It is noteworthy that an average 3°/2° value of 2.7 has been reported in 'gif type' of oxidation of adamantane [19]. In contrast, hydroxyl radical mediated oxidation of adamantane typically yields 3°/2° values close to 2.0 [20]. The normalized 3°/2° obtained in the present study are close to that obtained for structurally similar μ-oxo diiron(III) complex $[Fe_2O(bipy)_4(H_2O)_2](ClO_4)_4$ [21] . While for the $Fe(II)TPA(CH_3CN)_2/H_2O_2$ system it is 15-33 [22] and for the PhIO catalyzed P450 mimics it is 11-48 [23]. The enhanced regioselectivity with this catalyst using *m*-CPBA indicates the involvement of a metal-centered oxidant as an active intermediate in the oxidation of the C-H bonds of adamantane.

The exact mechanism for alkane hydroxylation with *m*-CPBA by the *μ*-oxo diiron(III) motifs is not completely clear to us. However, the sequence shown in Scheme II.2 seems probable. We propose that addition of *m*-CPBA to the diferric complexes generates benzoylperoxodiiron(III) species, $[Fe_2O(L_2)(OOCOC_6H_4Cl)]^{3+}$. This putative species can undergo either O-O bond homolysis or heterolysis leading

to the formation of high-valent iron(IV)-oxo or iron(V)-oxo species, which in turn oxidizes the substrate. The formation of high-valent oxoiron transient in the present case is also consistent with high A/K ratio during cycloalkane oxidation and moderately high 3°/2° ratio during oxidation of adamantane.

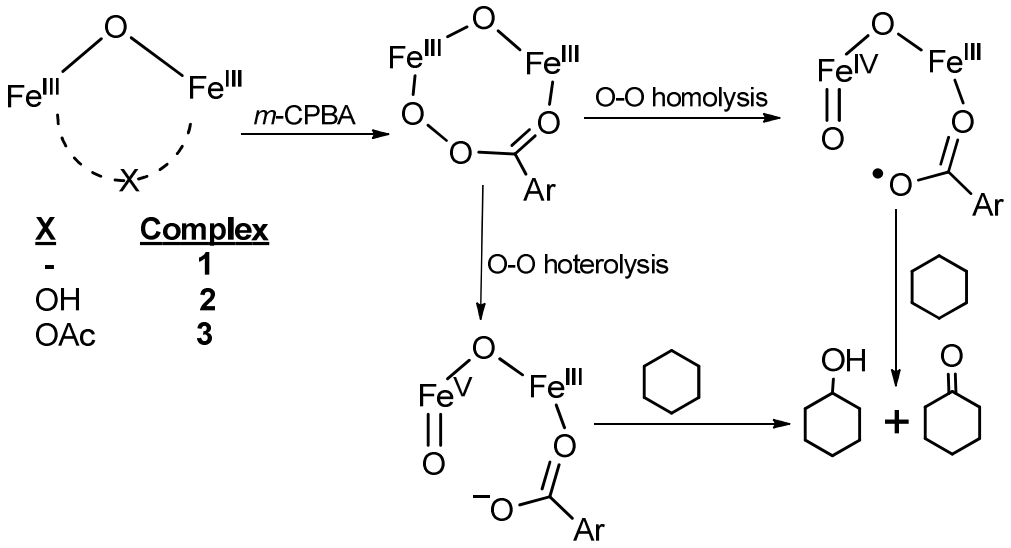

Scheme II.2 Plausible mechanism for alkane hydroxylation by the μ-oxo diiron(III)complexes (**1**-**3)** and *m*-CPBA.

II.2.3.2. Oxidation of alcohols

The reactivity of the μ-oxo diiron(III) cores towards alkanes with *m*-CPBA encouraged us to use mild and environmentally benign hydrogen peroxide as the oxidant. Akimova *et al.* have previously studied catalytic olefin epoxidation by the complexes **2** and **3** with H_2O_2 [15f]. Complex **3** has been found to be catalytically inactive while complex **2** afforded epoxides and trace amount of *cis*-diols. Therefore, in order to evaluate their ability towards catalytic hydroxylation, we attempted reactions of cycloalkanes with H_2O_2 in presence of the complexes (**1**-**3**). But apart from complex **2**, the other two complexes turn out to be inactive as less than 1% conversion of H_2O_2 into products has been obtained. However, the μ-oxo diiron(III) complexes have been found to catalyze oxidation of alcohols at room temperature with hydrogen peroxide. Their catalytic performance has been compared using benzyl alcohol as the substrate.

Table II.5 Oxidation of alcohols to carbonyl compounds by hydrogen peroxide catalyzed by complex **1** at room temperature[a].

Entry	Substrate	Catalyst	Products (% yield)[b]
1	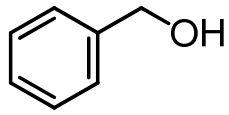	**1**	Benzaldehyde (90)
2		**2**	Benzaldehyde (65)
3		**3**	Benzaldehyde (60)
4	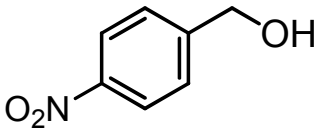	**1**	4-Nitro benzaldehyde (80)
5		**2**	4-Nitro benzaldehyde (100)
6		**3**	4-Nitro benzaldehyde (75)
7	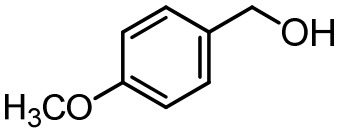	**1**	4-Methoxy benzaldehyde (70)
8		**2**	4-Methoxy benzaldehyde (60)
9		**3**	4-Methoxy benzaldehyde (50)

[a]Reaction Condition: 0.7mM catalyst, 700 mM substrate, 7 mM H_2O_2 in acetonitrile at room temperature; [b]Yields are reported with respect to the initial concentration of the oxidant

Interestingly, complex **1** has been found to promote oxidation of benzyl alcohol with significantly higher yield than **2** or **3** (Table II.5). While the catalytic performance of complex **3**, the so called 'thermodynamic sink' [24] is not surprising, somewhat lesser yield observed in the oxidation of benzyl alcohol to benzaldehyde catalyzed by complex **2** with H_2O_2 is unusual. However, when this reaction is followed by UV-Vis spectroscopy, formation of a band at 615 nm is observed and the solution turns blue-green (Fig II.7).

The spectroscopic feature is indicative of the formation of iron(III) complex bearing a 2-hydroxy benzyl alcohol ligand derived from the aromatic ring hydroxylation of benzyl alcohol at the *ortho* position (Scheme II.3).

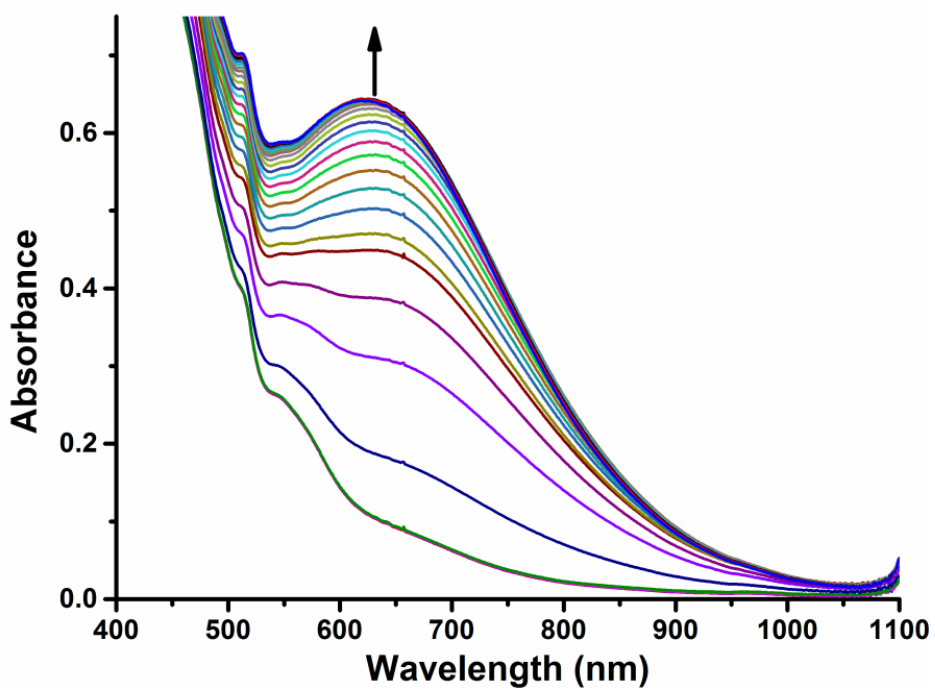

Fig II.7 UV-vis spectral changes in the reaction of 1.0 mM $[Fe_2(\mu\text{-}O)(\mu\text{-}OH)(bpmen)_2]$ (**2**) and H_2O_2 (10 mM) in presence of 100 mM benzyl alcohol in acetonitrile at 298K.

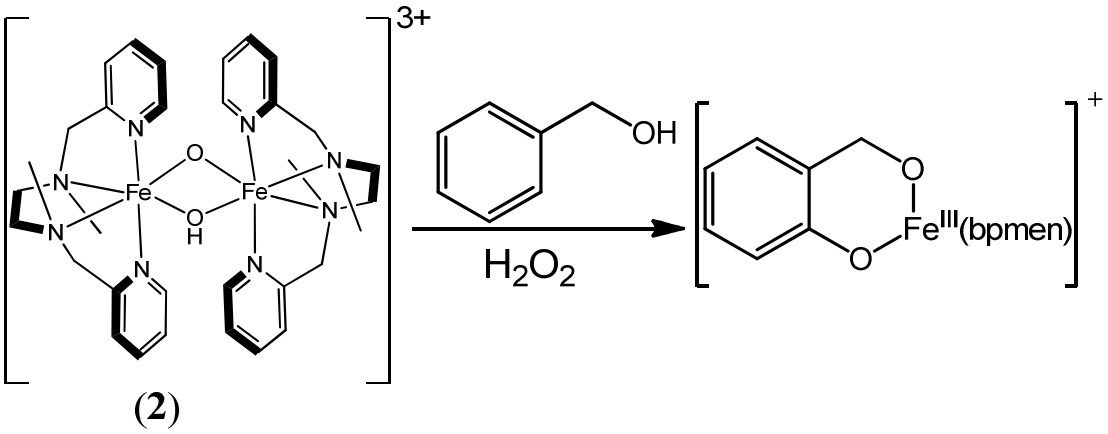

(**2**)

Scheme II.3 Ortho-hydroxylation of benzyl alcohol by **2**/H_2O_2.

Similar electronic changes have previously been observed in reactions between non-heme iron(II) complex $[Fe^{II}(bqen)]^{2+}$ (bquen = N,N'-dimethyl-N,N'-bis(8-quinolyl)ethane-1,2-diamine) peracetic acid and benzyl alcohol [25]. Complete absence of such iron(III) species in case of complex **1** and **3** suggests that only complex **2** is capable of hydroxylating the aromatic ring of benzyl alcohol. This is

further supported by the fact that in case of 4-nitro benzyl alcohol no aromatic hydroxylation is observed by **2**/H_2O_2 and the corresponding benzaldehyde is obtained quantitatively.

II.3. Conclusion

1. Catalytic activity of a group of μ-oxo bridged diferric complexes of bpmen ligand (**1**-**3**) differing in the Fe-O-Fe angles and the coordination environment around iron(III) towards alkane hydroxylation has been studied.

2. For the first time, it has been demonstrated that the diferric oxo-bridged complexes with bpmen ligand can catalyze the hydroxylation of alkanes at room temperature using *m*-CPBA.

3. Among the three diferric complexes, complex **1** is hitherto unknown. The complex (**1**) featuring a linear μ-oxo bridge was characterized by single crystal X-ray crystallography. Inert alkanes such as cyclohexane (BDE = 99 kcal/mol) and cyclooctane (BDE =96 kcal/mol) have been oxidized to the corresponding hydroxyalkanes with high selectivity (A/K=3.0-3.5). Complex **1** emerges as the best catalyst among the three μ-oxo diiron(III) complex complexes.

4. The diiron(III) complexes (**1**-**3**) are also effective in catalytic alcohol oxidation with environmentally benign H_2O_2 as the oxidant at room temperature. These results clearly demonstrate the catalytic potential of suitable μ-oxo diiron(III) complexes towards oxyfunctionalization of hydrocarbons under mild condition.

II.4. Experimental Section

II.4.1. Materials and physical methods

All chemicals were of reagent grade and were used without further purification. The exact oxygen content of H_2O_2 (30%w/v) and m-CPBA was determined iodometrically prior to use.The ligand N,N'-dimethyl-N,N'-bis(2-pyridylmethyl)-ethane-1,2-diamine) (bpmen) and the diiron complexes, *viz.*, $[Fe_2(\mu\text{-}O)(\mu\text{-}OH)(bpmen)_2]$ (**2)** and $[Fe_2(\mu\text{-}O)(\mu\text{-}CH_3COO)(bpmen)_2]$ **(3)** were prepared according to the published procedures [15, 11]. Elemental microanalyses (C, H and N) were done by either Perkin-Elmer (Model 240C) or Heraeus Carlo Erba 1108 elemental analyzer. Electronic spectra were recorded on an Agilent-5843 spectrophotometer. The ^{1}H NMR spectra were recorded on a Bruker spectrometer operating at 300 MHz. ESI-MS spectra were obtained on a Waters-Q-Tof premier-HAB213 mass spectrometer. Gas Chromatography (GC) analyses were performed on a Clarus-500 (PerkinElmer) GC instrument equipped with an FID detector.

II.4.2. Synthesis of the ligand

The ligand bpmen (bpmen = N,N'-dimethyl-N,N'-bis(2-pyridylmethyl)-ethane-1,2-diamine) was synthesized according to the following procedure [15a]. To a solution of (2-chloromethyl)-pyridine hydrochloride (3.0 g, 18.3 mmol) in water (10 mL) was added dropwise a solution of K_2CO_3 (5.1 g, 37 mmol) in water (15 mL). After stirring at room temperature for 30 min, the reaction mixture was extracted with CH_2Cl_2 (3x20 mL). The organic layers were combined, dried over Na_2SO_4, and concentrated in vacuo to afford orange oil. This free base product (2.2 g,17.5 mmol) was dissolved in CH_2Cl_2 (10 mL) and dropwise added to N,N'-dimethyl ethylene diamine (0.942 mL, 8.75 mmol) dissolved in CH_2Cl_2 (25 mL).After the slow addition of aq.1M NaOH (20 mL, 20 mmol), the resulting mixture was stirred for 60 h at room temperature, followed by rapid addition of a second fraction aqueous 1M NaOH (20 mL, 20 mmol).The aqueous layer was then extracted with CH_2Cl_2 (3x50 mL) and the combined organic layers were dreid over Na_2SO_4 to afford the bpmen as an orange oil. Yield: 1.6 g (68%). ^{1}H NMR (300 MHz, $CDCl_3$): δ = 2.27 (s, 6H, -N-CH_3), 2.66 (s, 4H, -CH_2-CH_2-), 3.69 (s, 4H, N-CH_2-Py), 7.1-8.54 (m, 8H, Py ring) ppm.

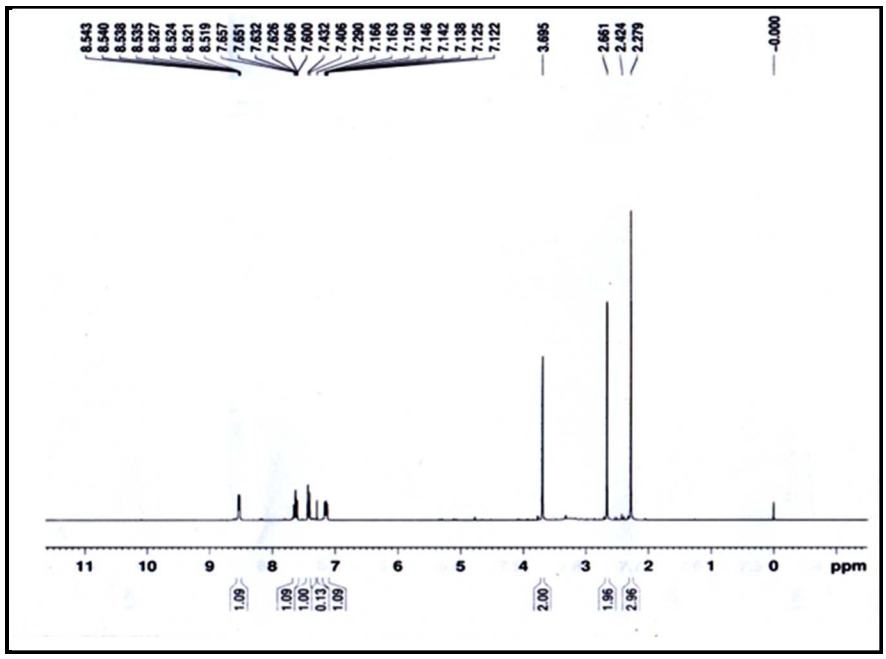

Fig II.8 ^{1}H NMR of the ligand bpmen in $CDCl_3$.

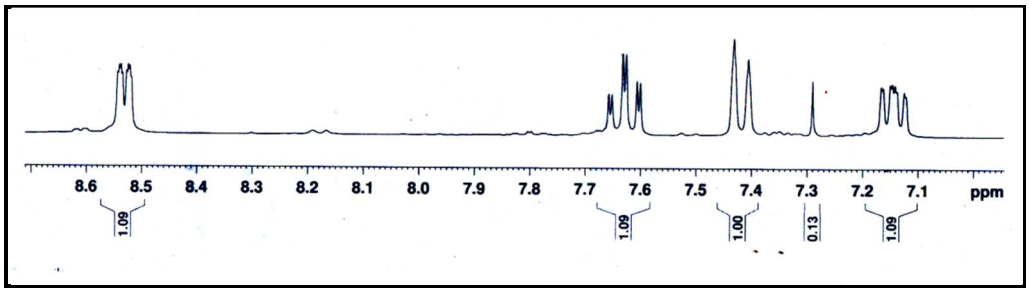

Fig II.9 ^{1}H NMR of the ligand bpmen in $CDCl_3$ (Expanded aromatic region).

II.4.3. Synthesis of the complees

II.4.3.1. Synthesis of [Fe(bpmen)(μ-O)$FeCl_3$] (**1**)

To a stirring solution of a 2.0 mL ethanolic solution containing the ligand bpmen (0.17 g, 0.629 mmol) a 2.0 mL solution of anhydrous $FeCl_3$ (0.102g, 0.629 mmol) in 2.0 mL ethanol was added. After the addition immediate precipitation of brown solid was observed. The precipitate was filtered and washed with diethyl ether and dried in vacuum.

Yield: 0.152 g (45%). Anal. Calc. for $C_{16}H_{22}Fe_2ON_4Cl_4$: C, 34.54; H, 4.33; N, 10.02. Found C, 34.58; H, 4.37; N, 10.3%. λ_{max}/nm (ε/M^{-1} cm^{-1}) = 269 (25,850), 339 (12,170), 400 (2,580).

II.4.3.2. Synthesis of [Fe(bpmen)(μ-O)(μ-OH)Fe(bpmen)](ClO$_4$)$_3$ (2)

The ligand bpmen (0.8 g, 2.962 mmol) was dissolved in 40 mL of ethanol/water (1:1 *v*/*v*) with sodium hydroxide (0.146 g, 3.658 mmol) and slowly added to a solution of Fe(ClO$_4$)$_3$.10H$_2$O (1.994 g, 3.72 mmol)) dissolved in 7 mL of ethanol. The mixture was left overnight in the refrigerator. Different batches led to the formation of a maroon powder.

Yield: 2.2 g (75%). ESI-MS: m/z : 392 (100%) [M-2ClO$_4$]$^{+2}$. Anal. Calc. for $C_{32}H_{45}N_8Fe_2Cl_3O_{14}$: C, 39.07; H, 4.61; N, 11.39. Found C, 38.39; H, 4.81; N, 11.26%.

II.4.3.3. Synthesis of [Fe(bpmen)(μ-O)(μ-OAc)Fe(bpmen)](ClO$_4$)$_3$ (3)

A mixture of bpmen ligand (400 mg, 1.48 mmol) and sodium acetate (121 mg, 1.48 mmol) dissolved in methanol (5 mL) and water (1 mL) was added to Fe(ClO$_4$)$_3$.10H$_2$O (793 mg, 1.48 mmol) dissolved in methanol (5 mL).The colour of the reaction mixture was changed to green and the product precipitated as fine brown powder. After stirring for 1 hour, the complex was collected by filtration and washed thoroughly with cold methanol, diethyl ether and finally air dried.

Yield: 900 mg (60%). ESI-MS: m/z : 413 [M-2ClO$_4$]$^{+2}$. λ_{max}/nm (ε/M^{-1} cm^{-1}) = 422(sh) (1100), 464 (1310), 495(sh) (860), 512(800), 543(sh) (230), 670(160). Anal. Calc. for $C_{34}H_{47}N_8Fe_2C1_30_{15}$: C, 39.80; H, 4.60; Cl, 10.30; N, 10.90. found C, 39.65; H, 4.45; Cl, 10.35; N, 10.95 %.

II.4.4. Catalytic reactions

Homogeneous catalytic oxidation reactions were carried out in small screw-capped vials fitted with PTFE septa. In a typical reaction 0.7 mM of catalyst and 700 mM of substrate were dissolved in 2 mL acetonitrile. The oxidation reaction was initiated by adding 7.0 mM of H_2O_2 and the contents were stirred by using magnetic bar. A standard solution of iodopentaflurobenzene was added to the reaction mixture as internal standard and an aliquot was injected into a preheated GC. The identification and the quantization of the products were done from the response factors of standard product samples as usual. In case of oxidation with *m*-CPBA, an acetonitrile solution (1.0 mL) of this oxidant (70 mM) was added to an acetonitrile solution (1.0 mL) of catalyst (0.7 mM) and alkane (700 mM) under nitrogen atmosphere with

vigorous stirring. After 1 h the iodopentaflurobenzene was added to the reaction mixture as an internal standard and directly analysed by GC. In case adamantane, CH_3CN-CH_2Cl_2 (2:3, *v*/*v*) was used as the solvent due to the poor solubility of adamantane in acetonitrile.

II.4.5. X-ray Crystallography

Single crystals of **1** were grown by slow diffusion of diethyl ether into an acetonitrile solution of the complex. Selected crystal data and data collection parameters are given in Table II.1. Data on the crystals were collected on a Bruker SMART 1000 CCD area-detector diffractometer using graphite monochromated MoKα (λ = 0.71073 Å) radiation by ω scan. The structure was solved by direct methods using SHELXS-97 [26] and difference Fourier syntheses and refined with SHELXL97 package incorporated in WinGX 1.64 crystallographic collective package [27]. All the hydrogen positions for the compound were initially located in the difference Fourier map, and for the final refinement, the hydrogen atoms were placed geometrically and held in the riding mode. The last cycles of refinement included atomic positions for all the atoms, anisotropic thermal parameters for all non-hydrogen atoms and isotropic thermal parameters for all the hydrogen atoms. Full-matrix-least-squares structure refinement against $|F^2|$. Molecular geometry calculations were performed with PLATON [28], and molecular graphics were prepared using ORTEP-3 [29].

CCDC-989145 contains the supplementary crystallographic data for this paper. These data can be obtained free of charge from The Cambridge Crystallographic Data Centre via www.ccdc.cam.ac.uk/data_request/cif.

References

1. L. Que, Jr., W. B. Tolman, *Angew. Chem. Int. Ed.*, 2002, **41**, 1114.
2. D. M. Kurtz, Jr., *Chem. Rev.* 1990, **90**, 585.
3. E.Y. Tshuva, S. J. Lippard, *Chem. Rev*, 2004, **104,** 987.
4. B. J. Wallar, J. D. Lipscomb, *Chem. Rev.* 1996, **96**, 2625.
5. M. Merkx, D. A. Kopp, M. H. Sazinsky, J. L. Blazyk, J. Müller, S. J. Lippard, *Angew. Chem. Int. Ed.*, 2001, **40**, 2782.
6. A. C. Rosenzweig, C. A. Fredrick, S. J. Lippard, P. Nordlund, *Nature*, 1993, **366**, 537.
7. A. Jordan, P. Reichard, *Annu. Rev. Biochem.*, 1998, **67**, 71.
8. D. T. Logan, X.-D. Su, A. Åberg, K. Regnström, J. Hajdu, H. Eklund, P. Nordlund, *Structure*, 1996, **4**, 1053.
9. J. A. Broadwater, J. Ai, T. M. Loehr, J. Sanders-Loehr, B. G. Fox, *Biochemistry*, 1998, **37**, 14664.
10. R. E. Norman, R. C. Holz, S. Ménage, C. J. O'Conor, J. H. Zhang, L. Que., Jr, *Inorg. Chem.*, 1990, **29**, 4629.
11. R. Hazell, K. B. Jensen, C. J. McKenzie, H. Toftlund, *J. Chem. Soc. Dalton Trans.* 1995, 707.
12. M. C. Esmelindro, E. G. Oestreicher, H. Márquez-Alvarez, C. Dariva, S. M. S. Egues, C. Fernandes, A. J. Bortoluzzi, V. Drago, O. A. C. Antunes, *J. Inorg. Biochem.*, 2005, **99**, 2054.
13. R. Khattar, M. S. Hundal, P. Mathur, *Inorg. Chim. Acta.*, 2012, **390**, 129.
14. G. Xue, R. De Hont, E. Münck, L. Que, Jr, *Nat. Chem.*, 2010, **2**, 400.
15. (a) A. Iturrospe, B. Artetxe, S. Reinoso, L. S. Felices, P. Vitoria, L. Lezama, J. M. Gutiérrez-Zorrilla, *Inorg. Chem*., 2013, **52**, 3084; (b) S. Taktak, S.V. Kryatov, E.V. Rybak-Akimova. *Inorg Chem*, 2004, **43,** 7196; (c) E. A. Duban, T. N. Drebushchak, K. P. Bryliakov, E. P. Talsi, *Mendeleev Commun.*, 2007, **17**, 291; (d) T. Okuno, S. Ito, S. Ohba, Y. Nishida *J. Chem. Soc. Dalton. Trans.*, 1997, 354; (e) S. Poussereau, G. Blondin, M. Cesario, J. Guilhem, G. Chottard, F. Gonnet, J. J. Girerd, *Inorg. Chem.*, 1998, **37**, 312; (f) S. Taktak, V. Kryatov, E. T. Haas, E. V. Rybak-Akimova, *J. Mol. Catal. A: Chemical*., 2006, **259**, 24.
16. M. C. White *Science*, 2012, **335**, 807
17. M. S. Chen, M. C. White, *Science*, 2010, **327**, 566.
18. O.V. Makhlynets, P. P. Das, S. Taktak, F. Margaret, M. B. Ruben, E. V. Rybak-Akimova, L. Que, Jr., *Chem. Eur. J.*, 2009, **15**, 13171.
19. D. H. R. Barton, J. Boivin, W. B. Motherwell, N. Ozabalik, K. M. Schwarzentruber, K. Jankowski, *New J. Chem.*, 1986, **10**, 387.
20. B. Singh, J. R. Long, F. F. De Biani, D. Gatteschi, P. J. Stavropoulos, *J. Am. Chem. Soc.*, 1997, **119**, 7030
21. S. Menage, J. M. Vincent, C. Lambeaux, M. Fontecave, *J. Chem. Soc. Dalton. Trans.*, 1994, 2081.
22. C. Kim, K. Chen, J. Kim, L. Que., Jr, *J. Am. Chem. Soc* ., 1997, **119**, 5964.
23. N. Kitajima, H. Fukui, Y. Moro-oka *J. Chem. Soc. Chem. Commun.*, 1988, 485.

24. R. E. Norman, S. Yan, L. Que, Jr., G. Backes, J. Ling, J. S. Loehr, J. H. Zhang, J. C. O'Connor, *J. Am. Chem. Soc.*, 1990, **112**, 1554.
25. J. Yoon, S. A. Wilson, Y. K. Jang, M. S. Seo, K. Nehru, B. Hedman, K. O. Hodgson, E. Bill, E. I. Solomon, W. Nam, *Angew. Chem. Int. Ed.*, 2009, **48**, 1257.
26. G. M Sheldrick SHELX97, University of Göttingen, Germany, 1997.
27. L. J. Farrugia, WinGX Version 1.64, An Integrated System of Windows Programs for the Solution, Refinement and Analysis of Single-Crystal X-ray Diffraction Data, Department of Chemistry, University of Glasgow, 2003.
28. PLATON: A. L. Spek , *J Appl Crystallogr.,* 2003, **36**, 7.
29. L. J. Farrugia, *J. Appl. Crystallogr.,* 1997, **30**, 565.